Eur. Phys. J. B **18**, 565–571 (2000)

THE EUROPEAN PHYSICAL JOURNAL B

EDP Sciences

Temperature renormalization of the magnetic excitations in S = 1/2 $KCuCl_3$

N. Cavadini[1,a], Ch. Rüegg[1], W. Henggeler[1], A. Furrer[1], H.-U. Güdel[2], K. Krämer[2], and H. Mutka[3]

[1] Laboratory for Neutron Scattering, ETH Zürich & Paul Scherrer Institut, 5232 Villigen PSI, Switzerland
[2] Department for Chemistry and Biochemistry, Universität Bern, 3000 Bern 9, Switzerland
[3] Institut Laue-Langevin, BP 156, 38042 Grenoble Cedex 9, France

Received 31 July 2000

Abstract. A complete temperature characterization of the spin dynamics in the unconventional $S = 1/2$ antiferromagnet $KCuCl_3$ is presented from single crystal inelastic neutron scattering studies. $KCuCl_3$ features a quantum disordered singlet ground state with a finite spin gap to triplet excitations of dimer origin. Three dimensional magnetic correlations support the dispersive propagation of the excitations in the whole reciprocal space. Upon increasing the temperature, a renormalization in the energy, in the intensity and in the damping rate of the triplet modes is reported. The experimental observations can be described within the framework of a selfconsistent dimer RPA theory, with no free parameters. The driving mechanism behind the model is the thermally activated decrease of the occupation difference $n_0 - n_1$ between singlet and triplet dimer states. This is the expression of kinematic constraints which are of minor importance for classical magnons in Néel ordered antiferromagnets. Implications for the temperature dependence of macroscopic quantities are discussed.

PACS. 75.30.Et Exchange and superexchange interactions – 75.10.Jm Quantized spin models – 78.70.Nx Neutron inelastic scattering

1 Introduction

The study of spin-spin correlations in unconventional $S = 1/2$ copper antiferromagnets (AF) remains at the forefront of solid state research. The reason for the continued interest in quantum magnetism relies both on the deep connection between layered Cu^{2+} antiferromagnets and high-T_c materials, as well as on the intrinsic nonlinearities and quantum fluctuations of low dimensional $S = 1/2$ systems. In this contribution we focus on the latter aspect and present a complete temperature analysis of the excitation spectrum in the $S = 1/2$ dimer compound $KCuCl_3$. The title compound already disposes of a comprehensive microscopic characterization, limited however to the lowest temperatures. Inelastic neutron scattering investigations determined that the magnetic interactions in $KCuCl_3$ result from a dominant AF bond J within pairs of nearest neighbor spins, which is accompanied by much weaker bonds J_{ij} to next nearest neighbors [1–3]. This creates a three-dimensional (3-D) network of copper dimers weakly linked together. Despite the true 3-D nature of the interdimer interactions, the intradimer coupling is sufficiently strong to impose a collective singlet ground state to the magnetic system. Opposite to the ordered Néel state of classical 3-D systems, the ground state in $KCuCl_3$ is quantum disordered as a result of spin fluctuations. A finite energy gap separates this nonmagnetic $S = 0$ ground state from dispersive $S = 1$ triplet excitations. Spin-spin correlations manifest themselves in form of a Bloch-like propagation of the triplet excitations, which coherently hop from one dimer site to the other according to the interdimer couplings previously determined [4]. At $k_B T \ll |J|$ the singlet-triplet excitations measured by inelastic neutron scattering are well defined modes. Their dispersion gives rise to an overall bandwidth centered at the intradimer excitation energy $|J| \sim 4.3$ meV and covering the energy range $\sim 2.7 - 5.0$ meV. Upon increasing the temperature, a characteristic flattening of the dispersion relation and a renormalization of the intensity is observed. A dimer model based on the random phase approximation (RPA) quantitatively accounts for both features. However, dimer RPA to lowest order predicts sharp excitations at all temperatures. This contradicts the experimental results which indicate a severe damping of the modes above the gap, obeying a thermally activated behaviour. Inclusion of higher order interdimer correlations in the diagrammatic RPA expansion is shown to well reproduce the observed damping, providing a useful paradigm to rationalize the complete temperature dependence of the spectral function $S(\kappa, \omega)$ with no free parameters.

[a] e-mail: nordal.cavadini@psi.ch

Detailed temperature studies on quantum AF are often limited in their temperature range by the stability of the magnetic phase under investigation. This is not the case for $KCuCl_3$, since the discussed unconventional spin properties are neither restricted to the low dimensionality of the spin Hamiltonian [5,6], nor related to lattice instabilities [7]. The dimer physics in $KCuCl_3$ is encoded in a three-dimensional Heisenberg model *a priori* [4], promoting the compound under investigation as an ideal candidate to study the interplay between quantum fluctuactions and thermal fluctuactions over a large $k_BT/|J|$ parameter range – for which a complete account is reported in the following. Section 2 of this contribution provides a self-contained summary of dimer RPA theory, tailored to the $KCuCl_3$ case. Experimental results are evaluated in light of this model in Section 3. Correlation expansions beyond simple dimer RPA are developed and successfully applied to explain the observed energy, intensity and linewidth dependence of the spectral function $S(\kappa,\omega)$. The agreement between model predictions and experimental data is satisfactory, considered that no free parameter is additionally introduced in the temperature analysis. In Section 4 the results are summarized and put into a more general context, including the parent compound $TlCuCl_3$.

2 Theory

Random Phase Approximation (RPA) has successfully been applied to describe crystal field excitations in a number of paramagnetic rare-earth compounds, where it accounted for the observed energy dispersion of the $4f$ crystal field excitations (see [8] for an overview). For the approach to be valid, the dynamic spin susceptibility χ of the system has to be dominated by smaller magnetic units, whose spin susceptibility χ_0 can exactly be expressed. The total susceptibility is then approximated as

$$\chi(\kappa,\omega) = \frac{\chi_0(\kappa,\omega)}{1 - J(q)\chi_0(\kappa,\omega)} \tag{1}$$

with $\kappa = q + \tau$ and ω corresponding to wave vector and energy, respectively in the usual notation. In the case of the $4f$ rare-earth ions, χ_0 is determined by the isolated crystal field single-ion spectrum and $J(q)$ is the Fourier transform of the additional exchange couplings between neighboring $4f$ sites.The same formalism can be adopted to explain the quantum interactions of $3d$ dimer systems [9], where however χ_0 describes the two-body dimer cluster rather than the single rare-earth ion

$$H_0 = -J \sum_i S_{i,1}\, S_{i,2} \tag{2}$$

and $J(q)$ is the Fourier transform of the effective exchange couplings J_{ij} between dimer pseudospins

$$H_1 = -\frac{1}{4} \sum_{ij} J_{ij}\ (S_{i,1} - S_{i,2})\,(S_{j,1} - S_{j,2}). \tag{3}$$

The indices i, j in the above equations represent different dimer sites, and roman numbers $1, 2$ single spins within the dimers. The expected energy of the singlet-triplet excitations is obtained from the poles of equation (1) by consideration of the exchange Hamiltonian expressed in equations (2) and (3). For a discussion of the effective dimer coupling scheme in $KCuCl_3$, we refer to the analysis presented in [3,4]. Two interconnected dimer sublattices are contained in the chemical unit cell. Accordingly, the resulting RPA energy dispersion reads

$$\epsilon_\pm(q) = \sqrt{J^2 + 2\ n(T) J J_\pm(q)}, \qquad n(T) = n_0 - n_1 \tag{4}$$

where the indices $\pm$ label the two excitation branches $\epsilon_+(q)$ and $\epsilon_-(q)$ observed in experiment [4], and $J_+(q), J_-(q)$ the corresponding Fourier transformations from equation (3). The thermal renormalization factor $n(T) = n_0 - n_1$ will be discussed below. Since the neutron measurements presented in this study have been collected on the a^*c^* scattering plane of $KCuCl_3$, the geometrical arrangement of the dimers implies that only the ϵ_+ branch can be detected. The complete RPA expression accounting for the complex spin susceptibility then reads

$$\chi''(\kappa,\omega) = \pi\ n(T)\ (\sin\frac{\kappa R}{2})^2 \frac{|J|}{\epsilon_+(q)}\ \delta(\hbar\omega - \epsilon_+(q)) \tag{5}$$

where $R = 0.48a + 0.32c$ is the projection on the ac plane of the spin-spin separation within the dimers [10], and the remaining notation has already been introduced. The characteristic dimer structure factor $(\sin\frac{\kappa R}{2})$ detailed in references [9,11] originates from the fact that two spins contribute to a dimer excitation. It modulates the intensity of the triplet modes according to the inelastic interference pattern experimentally reported for the $KCuCl_3$ compound in reference [2]. Equation (5) directly enters the inelastic neutron scattering cross section after

$$\frac{\mathrm{d}^2\sigma}{\mathrm{d}\Omega \mathrm{d}\omega}(\kappa,\omega) \sim \frac{\kappa_f}{\kappa_i}\ |f(\kappa)|^2 \frac{1}{1 - \mathrm{e}^{-\beta\hbar\omega}}\ \chi''(\kappa,\omega) \tag{6}$$

with $f(\kappa)$ denoting the magnetic form factor of the Cu^{2+} ion, κ_f and κ_i the final and initial neutron wavevector, respectively. The thermal renormalization factor $n(T) = n_0 - n_1$ introduced in equations (4, 5) corresponds to the weighted occupation difference between singlet and triplet dimer states, and has to be determined from the selfconsistent relation (see Refs. [12,13])

$$\frac{n_0 + n_1}{n_0 - n_1} = -\frac{1}{2N} \sum_q \left\{ \frac{J + n(T) J_+(q)}{\epsilon_+(q)} \coth\left(\frac{\epsilon_+(q)}{2k_BT}\right) + \frac{J + n(T) J_-(q)}{\epsilon_-(q)} \coth\left(\frac{\epsilon_-(q)}{2k_BT}\right) \right\} \tag{7}$$

under the canonical condition $n_0 + 3n_1 = 1$, where the sum in q runs over the irreducible Brillouin zone. The determination of the microscopic parameters by equations (4, 7) is known as self-consistent RPA. Neglecting the energy dispersion,

$$n_0 - n_1 = \frac{1 - \exp(-|J|/k_BT)}{1 + 3\exp(-|J|/k_BT)} \tag{8}$$

which corresponds to the Boltzmann occupation difference of uncorrelated singlet and triplet dimer states. Equation (8) vanishes for $k_BT \gg |J|$, where the singlet and triplet states are equally populated. At finite T it affects the spectrum by reducing the bandwidth of the energy dispersion, which is expected to flatten against the intradimer excitation limit $|J|$ as the temperature is increased, see equation (4). This allows an independent test for the strength of the leading parameter J of the spin system.

Unfortunately, the above RPA approach does not predict any damping of the excitation modes, for which additional terms in the diagrammatic expansion have to be considered. On the subject we remark that equation (1) is a special case of the general expression

$$\chi(\kappa,\omega) = \frac{\chi_0(\kappa,\omega)}{1-(J(q)-K(\omega))\chi_0(\kappa,\omega)} \tag{9}$$

where $K(\omega)$ renormalizes the bare exchange parameters as the result of the self energy of the correlated dimer system, *e.g.* the corrections due to the interdimer interactions [8]. The effect of K is to shift the poles of equation (9) both in the real axis (energy ϵ) as well as in the imaginary axis (damping Γ). The energy dispersion of the excitations retains the spectral expression presented in equation (4), albeit with screened parameters $J', J'(q)$ as formalized in references [12,13]. At the same time a finite lifetime of the excitations is predicted, whose damping rate Γ can be approximated as

$$\Gamma(\omega) = \frac{\pi}{2}\ \frac{n_0+n_1-(n_0-n_1)^2}{(n_0-n_1)^2}\ \left(\frac{J'^2-\omega^2}{\omega}\right)^2\ D(\omega) \tag{10}$$

where $D(\omega)$ is the selfconsistent density of states of the triplet modes, and J' the renormalized intradimer energy [8,12]. This approximation is valid as long as the relative change in the weighted energy $(\frac{J'^2-\omega^2}{\omega})^2 D(\omega)$ is small in the range determined by the width Γ. Appropriate corrections to equation (10) can be found in the cited literature, and are partly addressed in the following section. $\Gamma(\omega)$ itself directly scales after equation (10) with the fluctuactions of the renormalization factor $n(T) = n_0 - n_1$. From the model derivation, the leading mechanism for the damping of the triplet propagation is the loss of coherence due to the random fluctuactions of occupation numbers at each dimer site. Such magnetic scattering from single-site fluctuations is also discussed in [14]. The determination of the screened exchange couplings and of the damping rate along the lines addressed above does not introduce any additional free parameter, since the whole procedure is subject to sum rules discussed elsewhere [12,15,16].

3 Results

The renormalization of the magnetic excitations in $KCuCl_3$ was systematically investigated along selected directions in reciprocal space, covering the full bandwidth of the spectrum. From the inelastic neutron scattering spectra collected at different temperatures a strong renormalization of the energy, intensity and damping rate of the singlet-triplet modes is observed. In Figure 1, the measured energy dispersion and integrated intensity from constant κ-scans on the a^*c^* plane of $KCuCl_3$ is presented. For these scans, the spectrometers IN8, IN3 and IN22 at ILL (Grenoble) were operated at constant $E_f = 14.7$ meV under standard focusing conditions and a graphite filter in front of the analyzer. Results at $T \sim 2$ K provided reference values for the subsequent temperature investigations, performed under the same instrumental conditions. The energy dispersion at the lowest temperature (Fig. 1, continuous line at $T = 2$ K) is well described by the model parameters determined in [4], which also put the basis for the RPA analysis to be discussed. Upon increasing the temperature the dispersion relation is observed to flatten against the intradimer limit $|J|$, following the thermally activated renormalization quantitatively expected from the discussion of Section 2. Lines in Figure 1 correspond to the model expectations presented in equations (4, 5) at $T = 2$ K, $T = 19$ K and $T = 30$ K as indicated. The renormalization factor $n(T) = n_0 - n_1$ was approximated by the expression in equation (8), and evaluated at the appropriate temperature. The integrated intensity of the excitations at finite T is observed to characteristically decrease (Fig. 1, top panel). This behaviour is in accordance with equations (5, 6) on grounds of the kinematic limitations of the dimer unit, which forbid double

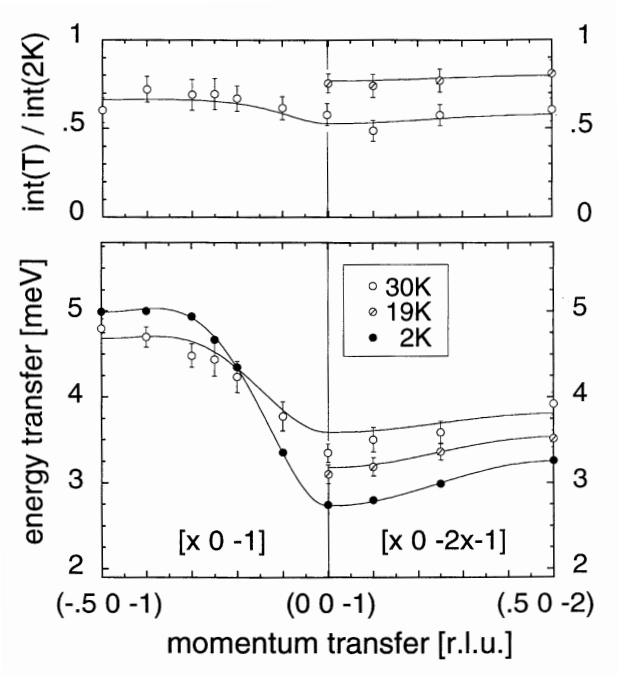

Fig. 1. Measured energy dispersion (bottom) and integrated intensity (top) of the magnetic excitations in $KCuCl_3$ at $T \sim 2$ K (full circles), $T \sim 19$ K (barred circles) and $T \sim 30$ K (open circles). Corresponding expectations are shown as continuous lines, according to the simplified RPA dimer model described in the text using equations (4) and (8).

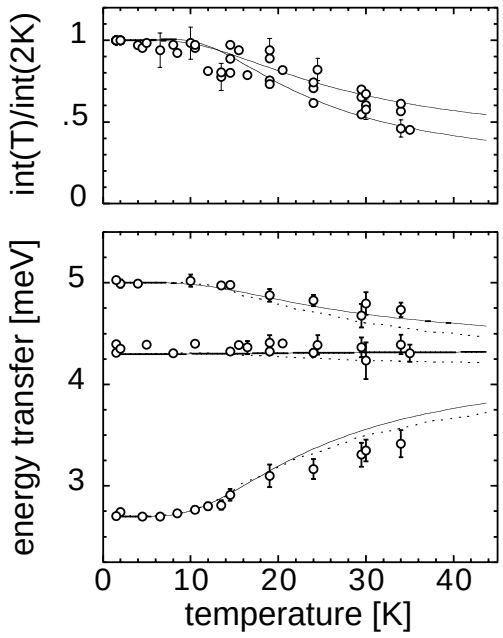

Fig. 2. Measured temperature renormalization of the energy (bottom) and integrated intensity (top) of the magnetic excitations in $KCuCl_3$ between $T \sim 2$ K and $T \sim 35$ K. Continuous lines in the bottom panel refer to the energy expectations from the simplified RPA dimer model described in equations (4) and (8) for modes starting at $\epsilon = 2.7,\ 4.3,\ 5.0$ meV at $T = 2$ K. Continuous lines in the top panel refer to the corresponding intensity expectations for the extremal modes, from equation (6). Dashed lines include the energy corrections from diagrammatic correlation expansions.

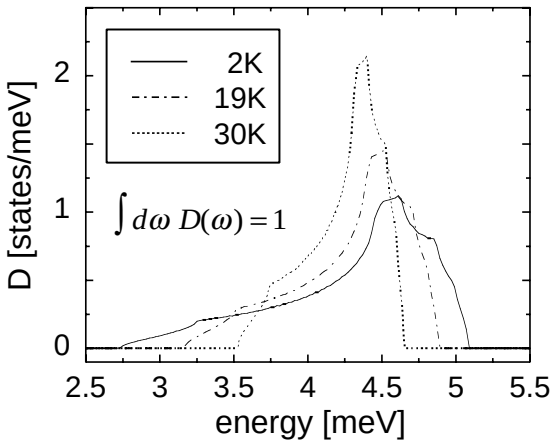

Fig. 3. Temperature dependence of the normalized density of states (d.o.s.) $D(\omega)$ determined from dimer correlation expansions. The d.o.s. corresponding to the continuous, dashed-dotted and dotted lines results from the model calculations performed at $T = 2$ K, $T = 19$ K and $T = 30$ K, respectively, as described in the text.

occupancy. Both the energy and the intensity RPA expectations follow with no free parameters with respect to the corresponding $T = 2$ K analysis. The overall agreement between model predictions and experimental observations is satisfactory, though not perfect. In particular, the mean field RPA approach discussed above seems to slightly overestimate the energy renormalization near to the minimum of the dispersion relation, where the reported effect is less pronounced than calculated. To clarify this issue, selected reciprocal points were investigated in a broad temperature range. Figure 2 summarizes the observed energy and integrated intensity up to $k_{\rm B}T \sim 3$ meV. The energy results (bottom panel) certify the stability of the magnetic interactions over the considered temperature interval, as indicated by the scans collected around the intradimer energy $|J|$, which does not markedly shift in energy. Moreover, they confirm the systematic inwards renormalization at the extrema of the dispersion relation. The observed behaviour of the integrated intensity in Figure 2 follows with reasonable accuracy the renormalization expected by RPA theory, whose boundary curves refer to the extremal modes from the bottom panel. Considered the stability of the leading exchange parameter J (Fig. 2, bottom panel), structural rearrangements are unlikely to be the reason for the spectral renormalization. Single crystal thermodynamic measurements up to room temperature certify the absence of any anomalies in this sense [17]. Rather, the reported effect occurs in $KCuCl_3$ within the framework of well defined magnetic interactions among dimerized Cu^{2+} pairs. RPA predicts such behaviour on a spin-only basis, as the result of the decrease in the weak interdimer correlations driven by the difference in the singlet-triplet thermal occupation $n_0 - n_1$. However, excitations from equation (5) are sharp at any temperature since the population difference on each dimer site is frozen in a mean-field *ansatz*. As it is shown in the following, an extension to include dynamic interdimer correlations can satisfactorily overcome this shortcoming, providing a useful paradigm to organize the energy, intensity and damping data on a common quantitative basis.

The determination of the microscopic RPA parameters within correlation theory follows the procedure described in reference [12] and first adapted to the dimer case in reference [13]. For our purposes, the density of states $D(\omega)$ of the triplet modes at $T = 2$ K was selfconsistently evaluated from the analysis presented in reference [4] (Fig. 3), by discretizing the irreducible reciprocal space in 10^6 points and enforcing the monotopic condition [13]

$$\frac{1}{2N}\sum_q \left\{ \frac{n(T)J'_+(q)}{\epsilon_+(q)} \coth\left(\frac{\epsilon_+(q)}{2k_{\rm B}T}\right) + \frac{n(T)J'_-(q)}{\epsilon_-(q)} \coth\left(\frac{\epsilon_-(q)}{2k_{\rm B}T}\right) \right\} = 0. \quad (11)$$

The temperature renormalization of the spectrum starting from the 2 K data is uniquely determined by the implicit set of equations (4, 7) (expressed as a function of $J', J'(q)$) under the condition in equation (11). Convergence is rapidly reached at each temperature step, since the interdimer correlations in $KCuCl_3$ are much weaker

Table 1. Comparison between the calculated (cal) and observed (obs) damping rates Γ for the excitation modes in $KCuCl_3$ at $T \sim 19$ K and $T \sim 30$ K. The considered points $\kappa = (h, k, l)$ in reciprocal lattice units (r.l.u.) refer to Figures 1 and 2, providing a complete sampling of the energy bandwidth of the excitations (from the top to the bottom). Calculations are the results of equation (10) as described in the text, with further comments to be found in Section 3.

$h\ k\ l$ [r.l.u.]			$\Gamma_{19\ \mathrm{K}}$ [meV]		$\Gamma_{30\ \mathrm{K}}$ [meV]	
$\epsilon/\lvert J\rvert < 1$:			cal	obs	cal	obs
0.00	0.00	−1.00	0.20	0.29(12)	0.61	0.54(16)
0.10	0.00	−1.20	0.27	0.40(16)	0.70	0.96(26)
0.25	0.00	−1.50	0.51	0.57(19)	1.12	0.90(26)
0.50	0.00	−2.00	0.62	0.42(17)	1.38	0.72(24)
−0.10	0.00	−1.00	0.58	–	1.34	1.01(17)
$\epsilon/\lvert J\rvert \sim 1$:						
−0.20	0.00	−1.00	[0.02]	–	[0.04]	0.84(22)
0.70	0.00	0.00	[0.04]	0.48(10)	[0.09]	1.05(17)
$\epsilon/\lvert J\rvert > 1$:						
−0.30	0.00	−1.00	0.63	–	1.44	0.55(25)
−0.50	0.00	−1.00	0.54	0.30(15)	1.18	0.75(21)
−0.40	0.00	−1.00	0.41	–	1.06	0.57(20)

than the intradimer correlation. As a result of the above corrections the calculated temperature renormalization at the bottom of the dispersion relation is closer to the experimental observations (Fig. 2). The evaluation of the expected damping rate Γ by the same microscopic approach yields the data summarized in Table 1. The model calculations from equation (10) (weighted in 0.1 meV energy bins) are compared to the experimental observations at the corresponding reciprocal points (from Figs. 1, 2). Considering that no free parameters are available, the values of Γ are in good agreement with the experimental data at $T = 19$ K, but less accurate at $T = 30$ K. Moreover, at excitation energies around $\epsilon \sim |J'|$ strong discrepancies are observed. The above features are commented below. Typical neutron profiles taken at $T \sim 2$ K and $T \sim 30$ K are reproduced in Figure 4 (IN8 at ILL). The effect of the dispersion relation on the instrumental resolution has been considered by full 4D convolution and found to be well described by Gaussian profiles, as confirmed by the experimental outcome (Fig. 4, horizontal bar). Scans at the same reciprocal points were evaluated by imposing common background conditions. Starting from the results at $T \sim 2$ K, the subsequent energy, intensity and linewidth of the excitations can thus be compared with no free parameters to the model predictions as reported in Figures 1, 2 and Table 1. Considering the large experimental body presented, good agreement is found for the complete information which can be extracted from the neutron profiles. An exception is provided by the excitations at $\epsilon \sim |J'|$, whose damping from equation (10) is predicted to vanish (Tab. 1, in brackets). This discrepancy is understood as the result of the truncation in the correlation expansions. In reference [8] a suitable correction is proposed, where

$$\Gamma(\omega) = \frac{2}{\pi}\ \frac{n_0 + n_1 - (n_0 - n_1)^2}{(n_0 - n_1)^2}\ \frac{1}{D(\omega)},\ \omega \sim |J'| \quad (12)$$

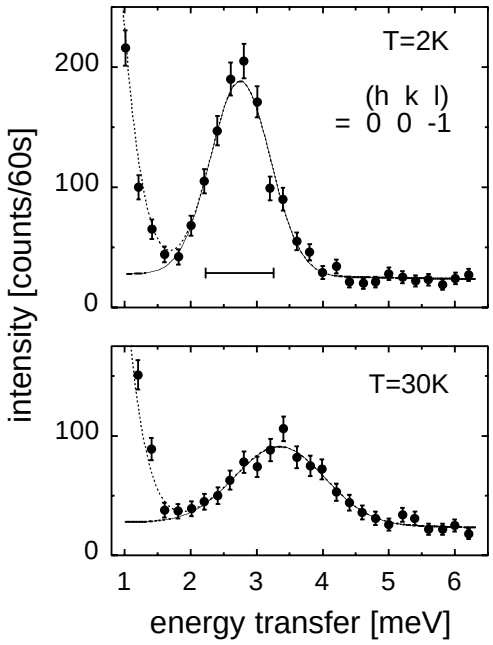

Fig. 4. Typical neutron profiles in $KCuCl_3$ at $T \sim 2$ K and $T \sim 30$ K, measured at the reciprocal point $\kappa = (0\ 0\ -1)$ [r.l.u.]. The observed energy, intensity and linewidth renormalization of the magnetic excitation mode is representative of the effects discussed in the text. The intensity excess at low energy transfers is due to the flanks of the elastic line, the horizontal bar indicates the instrumental resolution.

should replace equation (10) in the energy region of interest. The determination of the resulting damping follows the calculation scheme described above, yielding $\Gamma_{19\ \mathrm{K}} = 0.49$ meV and $\Gamma_{30\ \mathrm{K}} = 1.14$ meV, in much better agreement with the experimental observations (Tab. 1).

We remark however that the model at $T = 30$ K is likely to overestimate the actual damping rates. At this temperature in fact the expected linewidths are comparable to the overall bandwidth of the spectrum (Fig. 3), invalidating the assumptions discussed in Section 2. Highly resolved neutron investigations would clearly be of advantage in order to test more stringent predictions, in particular for the triplet modes at extrema of the excitation band and around the intradimer excitation energy as addressed for example in references [8,14].

To sum up, correlation theory qualitatively matches the characteristic energy and intensity renormalization also predicted by a dimer mean field RPA approach, stressing the validity of the dimer model in the description of $KCuCl_3$. The driving mechanism behind the thermally activated flattening of the dispersion is in both theories the decrease in the difference of the intradimer singlet-triplet occupation $n(T) = n_0 - n_1$. This behaviour is observed in other dimer systems, as exemplified by the energy and intensity analysis presented from neutron investigations of $S = 3/2$ Cr^{3+} dimers [9,13] and of $S = 1/2$ Cu^{2+} dimers [18,19]. In the latter study the momentum dependence of the damping rate of the singlet-triplet modes has been discussed on a phenomenological basis. Microscopic insights about the triplet dynamics can as well be derived from the field and temperature dependence of the NMR spin-lattice relaxation rate, as recently proven in a comprehensive experimental work [20]. In the present contribution dimer-correlation theory is shown to reproduce to a large extent the observed neutron spectra of the excitations in $KCuCl_3$, with no free parameters. Overcoming mean field RPA theory, it is proposed as a valuable paradigm to describe the dynamic magnetic properties of a nearly ideal 3-D spin liquid around the dimer limit, within a selfconsistent theoretical framework including kinematic interactions.

We conclude by noticing that the temperature induced microscopic change in the spectrum also affects macroscopic observables. The most sensitive quantity is the magnetization, which at $T = 0$ vanishes up to the critical field $g\mu_B H_c \sim \Delta$, where Δ denotes the spin gap in the spectrum. An immediate consequence of the increase of the gap energy $\Delta(T)$ with temperature (Figs. 1, 2) is for instance the increase of the critical field $H_c(T)$, which has been reported in both singlet-triplet compounds $KCuCl_3$ and $TlCuCl_3$ from high-field magnetization results [21,22]. This behaviour cannot be reproduced by simple macroscopic arguments, since it relies after Section 2 on the suppression of the interdimer correlations. In a recent study, the above H_c dependence on the temperature in $TlCuCl_3$ was interpreted as the possible indication of Bose-Einstein condensations of the triplet excitations upon approaching the quantum critical point H_c [23]. Apparently RPA theory provides an alternative explanation to the measurements, which is within the model proposed of kinematic nature only. Detailed temperature investigations of the spin-spin dynamics in $TlCuCl_3$ will hopefully help to elucidate the above topic.

4 Conclusions

A complete temperature analysis of the singlet-triplet quantum excitations in the $S = 1/2$ antiferromagnet $KCuCl_3$ has been presented. The ground state of this unconventional insulator is characterized by the absence of Néel static order, despite the three-dimensional nature of the spin-spin interactions. A quantum disordered singlet state is retained down to the lowest temperature due to a dominant AF bond, along which neighboring spins dimerize. Above a finite magnetic excitation gap, well defined singlet-triplet modes of dimer origin propagate in the whole reciprocal space. The energy, the spectral weight and the damping rate of these modes is observed to severely renormalize with temperature. The experimental observations are reproduced on a self-consistent basis by an RPA theory including kinematic corrections. Taking the microscopic excitation parameters from the observed dispersion relation at $T \sim 2$ K, the subsequent renormalization of the scattering function $S(\kappa, \omega)$ can be accounted for with no adjustable variables. This is interpreted as indication that relaxation processes to lowest order are triggered by scattering on single-site fluctuations in the dimer singlet-triplet occupation. On a macroscopic level the change in the spectrum is proposed to explain the anomalous $H_c(T)$ critical field behaviour reported for both isostructural $KCuCl_3$ and $TlCuCl_3$, and subject of recent experimental and theoretical studies. Joint temperature and field investigations with neutrons in $TlCuCl_3$ are anticipated, to map the phase diagram microscopically and to determine the unconventional spin-spin dynamics in the vicinity of a quantum phase transition.

Fruitful discussions with B. Braun, S. Haas, P. Lemmens, B. Normand, and M.E. Zhitomirsky are appreciated. The experimental support of L.P. Regnault during the IN22 measurements is gratefully acknowledged. This work was financially supported by the Swiss National Science Foundation.

References

1. T. Kato, K. Takatsu, H. Tanaka, W. Shiramura, M. Mori, K. Nakajima, K. Kakurai, J. Phys. Soc. Jpn **67**, 752 (1998).
2. N. Cavadini, W. Henggeler, A. Furrer, H.U. Güdel, K. Krämer, H. Mutka, Eur. Phys. J. B **7**, 519 (1999); Physica B **276-278**, 540 (2000).
3. T. Kato, A. Oosawa, K. Takatsu, H. Tanaka, W. Shiramura, K. Nakajima, K. Kakurai, J. Phys. Chem. Solids **60**, 1125 (1999).
4. N. Cavadini, G. Heigold, W. Henggeler, A. Furrer, H.U. Güdel, K. Krämer, H. Mutka, J. Phys. Cond. Matt. **12**, 5463 (2000).

5. D.A. Tennant, R.A. Cowley, S.E. Nagler, A.M. Tsvelik, Phys. Rev. B **52**, 13368 (1995).
6. D.A. Tennant, S.E. Nagler, D. Welz, G. Shirane, K. Yamada, Phys. Rev. B **52**, 13382 (1995).
7. M. Arai, M. Fujita, M. Motokawa, J. Akimitsu, S.M. Bennington, Phys. Rev. Lett. **77**, 3649 (1996).
8. J. Jensen, A.R. Mackintosh, *Rare Earth Magnetism, Structure and Excitations* (Clarendon Press, Oxford 1991).
9. B. Leuenberger, A. Stebler, H.U. Güdel, A. Furrer, R. Feile, J.K. Kjems, Phys. Rev. B **30**, 6300 (1984).
10. R.D. Willett, C. Dwiggins, R.F. Kruh, R.E. Rundle, J. Chem. Phys. **38**, 2429 (1963).
11. A. Furrer, H.U. Güdel, Phys. Rev. Lett. **39**, 657 (1977).
12. J. Jensen, J. Phys. C **15**, 2403 (1982).
13. B. Leuenberger, H.U. Güdel, J. Phys. C **18**, 1919 (1985).
14. P. Bak, Phys. Rev. B **12**, 5203 (1975).
15. D.H.Y. Yang, Y.L. Wang, Phys. Rev. B **12**, 1057 (1975).
16. S.B. Haley, P. Erdös, Phys. Rev. B **5**, 1106 (1972).
17. H. Tanaka, K. Takatsu, W. Shiramura, T. Ono, J. Phys. Soc. Jpn **65**, 1945 (1996).
18. Y. Sasago, K. Uchinokura, A. Zheludev, G. Shirane, Phys. Rev. B **55**, 8357 (1997).
19. G. Xu, C. Broholm, D.H. Reich, M.A. Adams, Phys. Rev. Lett. **84**, 4465 (2000).
20. G. Chaboussant, M.H. Julien, Y. Fagot-Revurat, M.E. Hanson, L.P. Lévy, C. Berthier, M. Horvatić, O. Piovesana, Eur. Phys. J. B **6**, 167 (1998); Phys. Rev. Lett. **80**, 2713 (1998).
21. W. Shiramura, K. Takatsu, H. Tanaka, K. Kamishima, M. Takahashi, H. Mitamura, T. Goto, J. Phys. Soc. Jpn **66**, 1900 (1997).
22. A. Oosawa, M. Ishii, H. Tanaka, J. Phys. Cond. Matt. **11**, 265 (1999).
23. A. Nikuni, M. Oshikawa, A. Oosawa, H. Tanaka, Phys. Rev. Lett. **84**, 5868 (2000).